Supporting Information

Metal-Organic Framework (MOF) Derived Recyclable, Superhydrophobic Composite of Cotton Fabrics for the Facile Removal of Oil Spills

*Rana Dalapati, Soutick Nandi, Chiranjib Gogoi, Arpita Shome and Shyam Biswas**

Department of Chemistry, Indian Institute of Technology Guwahati, Guwahati, 781039 Assam, India

* To whom correspondence should be addressed. E-mail: sbiswas@iitg.ac.in; Tel: 91-3612583309.

Movie S1: Hydrophobicity of **SH-UiO-66@CFs**

Movie S2: Absorption-based selective oil/water separation of heavy oils by **SH-UiO-66@CFs**

Movie S3: Absorption-based selective oil/water separation of light oils by **SH-UiO-66@CFs**

Movie S4: Filtration-based selective oil/water separation by **SH-UiO-66@CFs**

Movie S5: Collection of the underwater oil against gravity by **SH-UiO-66@CFs**

Materials and Physical Measurements. All the reagent grade starting materials and solvents were used without further purification as received from commercial suppliers. Perkin Elmer Spectrum Two FT-IR spectrometer was used to record Fourier transform infrared spectra in the range of 440-4000 cm^{-1}. To describe the FT-IR absorption bands, the following standard classifications were used: weak (w), very strong (vs), strong (s), medium (m), broad (br) and shoulder (sh). A Bruker D2 Phaser X-ray diffractometer working at 30 kV, 10 mA was employed for the collection of ambient temperature X-Ray powder diffraction (XRPD) patterns using Cu-Kα (λ = 1.5406 Å) radiation. A Mettler-Toledo TGA/SDTA 851e thermogravimetric analyzer was used for conducting the thermogravimetric analyses in the temperature range of 25-700 °C under air atmosphere with a heating rate of 5 °C min^{-1}. Quantachrome Autosorb iQ-MP gas sorption analyser was utilized for the nitrogen sorption experiments at -196 °C up to 1 bar. A Bruker Avance III 600 spectrometer was utilized for recording ^{1}H-NMR at 600 MHz. The mass spectrum (in ESI mode) was measured with an Agilent 6520 Q-TOF high-resolution mass spectrometer Contact angle experiments were performed by employing a KRUSS Drop Shape Analyzer-DSA25 instrument with an automatic liquid dispenser at ambient temperature. Field emission - scanning electron microscopy (FE-SEM) images were collected by Zeiss (Zemini) scanning electron microscope. Cotton was purchased from local medical shop of Guwahati city (Assam, India). Kerosene oil and gasoline were purchased from a local shop of Guwahati city (Assam, India). Digital images were captured using a Nikon Coolpix B500 digital camera.

Synthesis of 2-Trifluoroacetamidoterephthalic Acid (H_2L) Ligand. In a 50 mL round bottom flask, 1.81 g (10 mmol) of 2-aminoterephthalic acid was added slowly in 15 mL of trifluoroacetic anhydride at room temperature and the reaction mixture was stirred for 4 h. After that the reaction mixture was slowly poured in 20 mL of ice-cold water and a white precipitate appeared. The obtained white solid product of 2-trifluoroacetamidoterephthalic acid (H_2**L**) was filtered and washed with large amount of water. Yield: 69% (1.89 g, 6.9 mmol). ^{1}H-NMR: δ 12.57 (s, 1H), 8.78 (s, 1H), 8.13 (d, 1H), 7.88 (d, 1H) ppm; ^{13}C NMR: δ 169.14, 166.48, 155.25, 137.85, 135.87, 131.99, 126.31, 123.44, 122.38, 116.92, 115.00 ppm; ^{19}F NMR: δ -75.20 ppm. ESI-MS (m/z): 300.0140 for $(M+Na)^+$ ion (M = mass H_2**L** ligand). The NMR and mass spectra of H_2**L** ligand are shown in Figures S1-S4 (Supporting Information).

Absorption Capacities for Various Oils by SH-UiO-66@CFs Composite. In the oil absorption test, pre-weighed (~10-15 mg) hydrophobic **SH-UiO-66@CFs** composite was placed in 10 mL of various heavy oils (dichloromethane, chloroform and carbon tetrachloride) and light oils (ethyl acetate, toluene, hexane, motor oil, silicone oil, gasoline and kerosene) for

1 min to reach absorption equilibrium and then removed and weighed. All the experiments were made at room temperature. The absorption capacity (wt%) is defined as:

Absorption capacity (wt%) = $(W_4 - W_3)/W_3 \times 100\%$

The absorption capacity in (g/g) unit is defined as:

Absorption capacity (g/g) = W_4/W_3

where, W_3 is weight of oven-dried **SH-UiO-66@CFs** and W_4 is the weight of oil-absorbed **SH-UiO-66@CFs**. At least 10 measurements were carried out for each oil sample and the average value was plotted.

Absorption Based Separation of Oil and Water by SH-UiO-66@CFs Composites. For the separation of light oil from oil/water mixture, single piece of **SH-UiO-66@CFs** (~ 100-120 mg) was exposed to different oil/water mixtures that composed of 5 mL of oil and 40 mL of water. The oil phase was immediately soaked in **SH-UiO-66@CFs** and the separated oil was collected by squeezing the material manually. On the other hand, for the separation of heavy oil from oil/water mixture, a piece of **SH-UiO-66@CFs** (~ 100-120 mg) was brought into contact with the sediment oil. The modified cotton selectively absorbed the oil phase after coming into contact with the oil phase. All the experiments were performed at room temperature. The separation efficiency (%) is defined as:

Separation efficiency (%) = $V_2/V_1 \times 100\%$

where, V_1 is the volume of oil (mL) used and V_2 is the absorbed volume of oil (mL) by **SH-UiO-66@CFs**. Ten measurements were carried out for each oil sample and the average value was plotted.

Absorption Based Separation of Oil and Water by SH-UiO-66@CFs Composite under Different Conditions. This oil/water absorption-based separation process was further extended with several complex aqueous phases, such as tap water, lake water, river water, artificial sea water and water having different pH (2 and 12). Tap water was collected from IIT Guwahati campus, water of IIT Guwahati lake was used as lake water, water of Brahmaputra river (Assam, India) was utilized as river water. The artificial sea water was prepared by mixing $MgSO_4$ (0.325g), $MgCl_2$ (0.226g), $CaCl_2$ (0.112 g) and NaCl (2.673g)) in 100 mL deionized water in a volumetric flask. Motor oil was used as model oil for this experiment.

Reusability of SH-UiO-66@CFs. Mechanical squeezing by finger was used to extract the absorbed oil from the **SH-UiO-66@CFs**. The absorbed recovered oil was used again without any post-treatment. After collecting the oil from **SH-UiO-66@CFs**, the material was washed with THF to remove rest of the oil and heated in air oven at 80 °C for 2 h. The oven dried **SH-UiO-66@CFs** material was used further for the next set of oil absorption experiments.

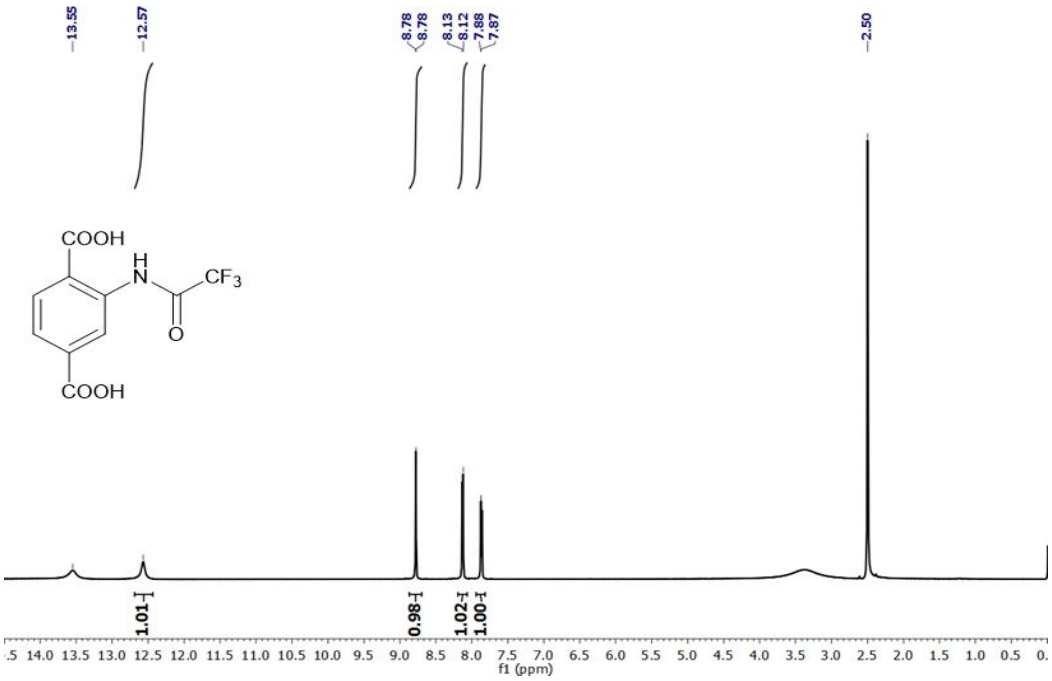

Figure S1. ^{1}H NMR spectrum of H_2**L** ligand measured in DMSO-d_6.

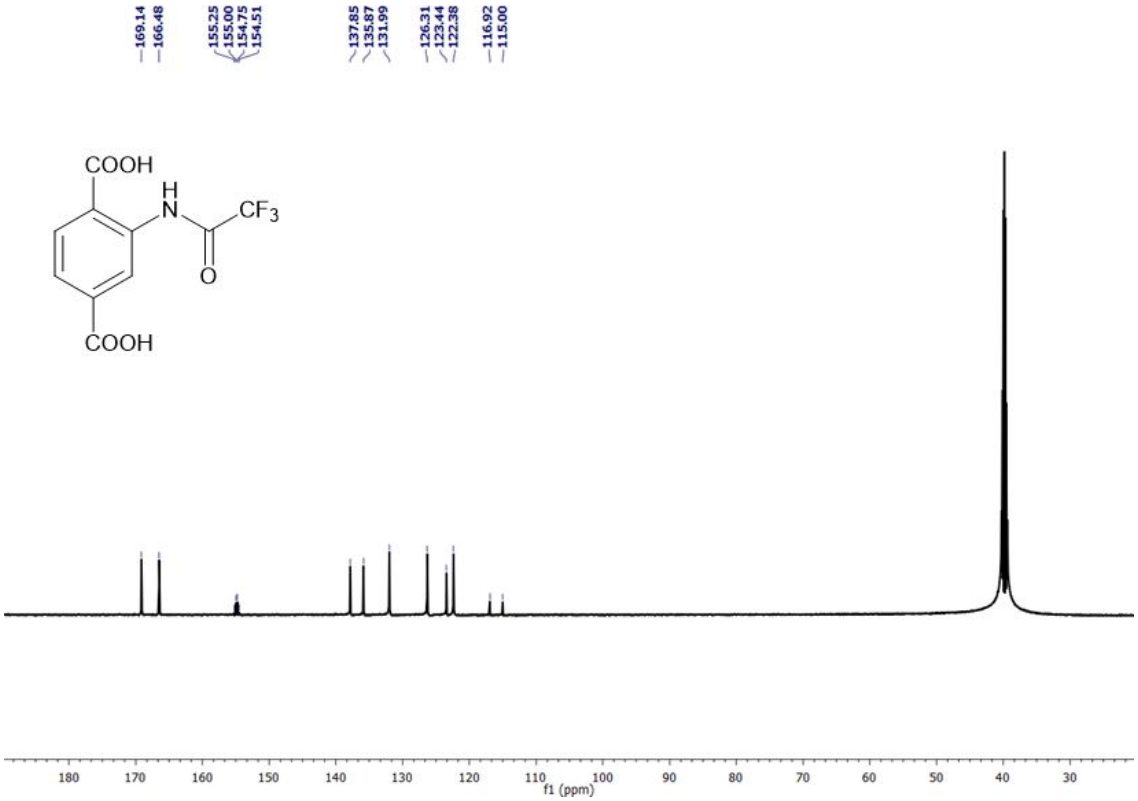

Figure S2. ^{13}C NMR spectrum of H_2**L** ligand measured in DMSO-d_6.

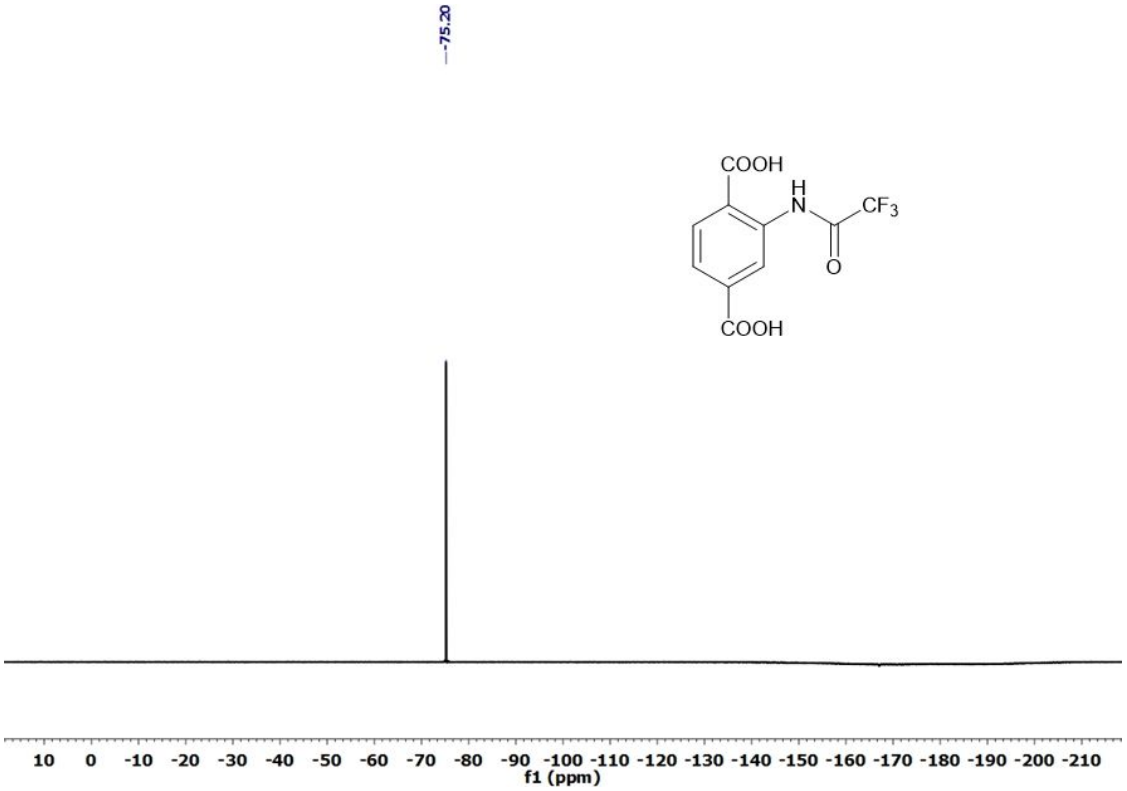

Figure S3. ^{19}F NMR spectrum of H_2**L** ligand measured in DMSO-d_6.

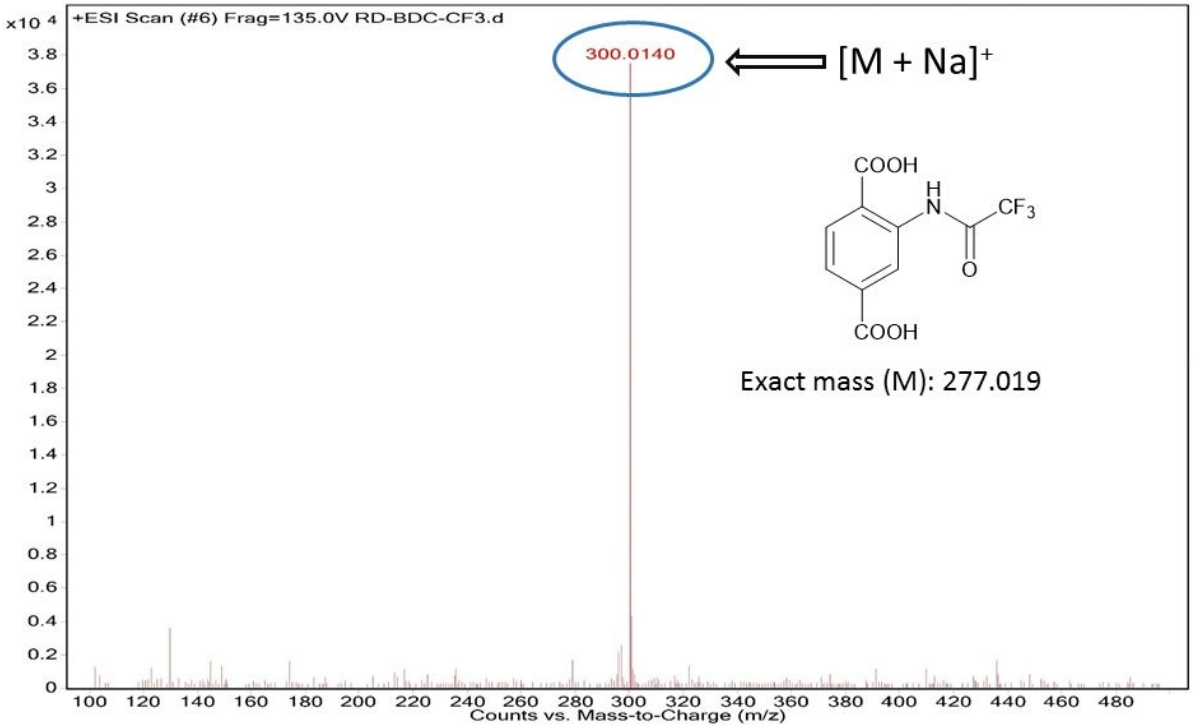

Figure S4. ESI-MS spectrum of H_2**L** ligand $(M + Na)^+$ measured in methanol.

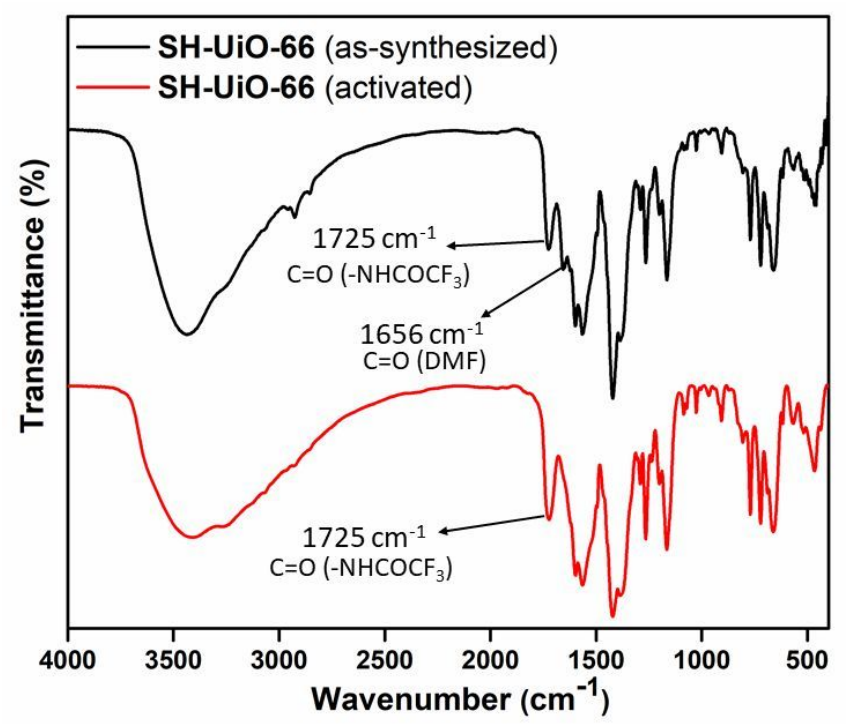

Figure S5. FT-IR spectra of as-synthesized (black) and thermally activated (red) form of **SH-UiO-66**.

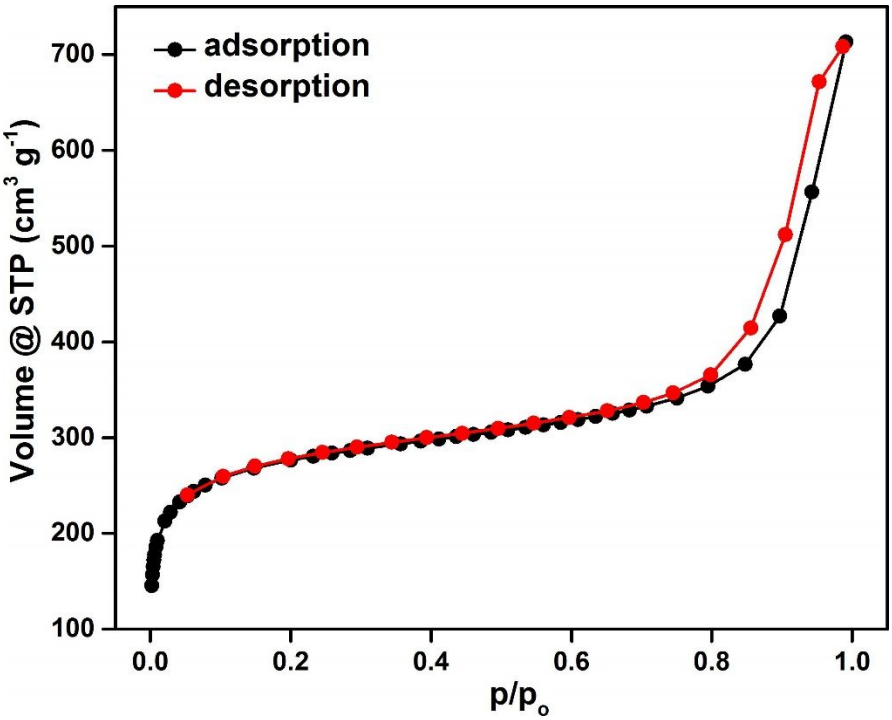

Figure S6. N_2 adsorption (black circles) and desorption (red circles) isotherms of activated **SH-UiO-66** recorded at –196 °C.

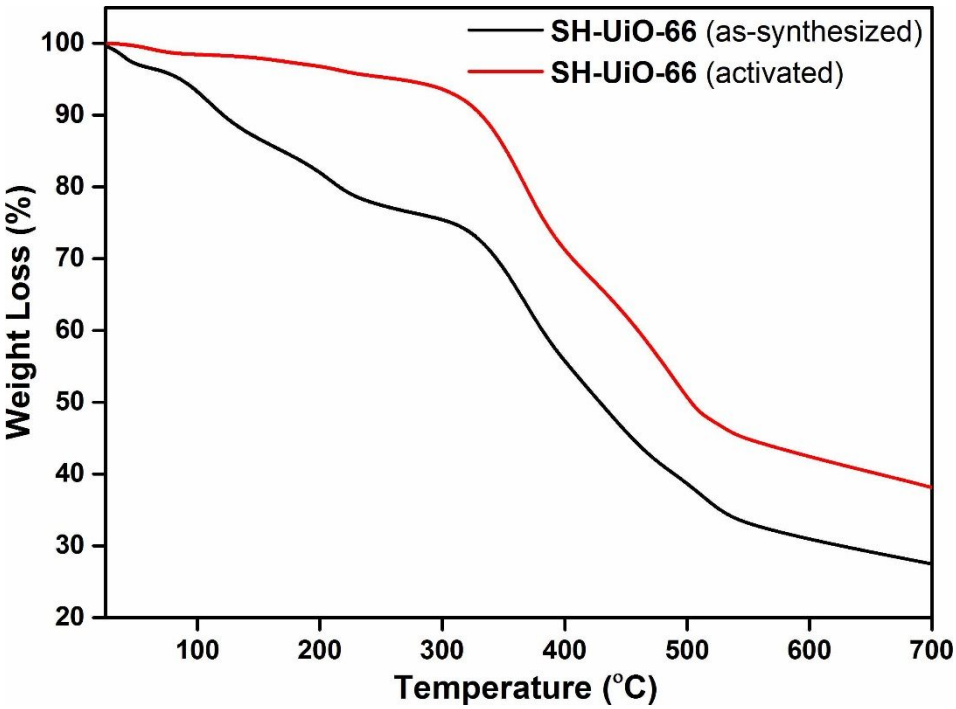

Figure S7. TG curves of as-synthesized and activated **SH-UiO-66** recorded in an air atmosphere in the temperature range of 25-700 °C with a heating rate of 5 °C min^{-1}.

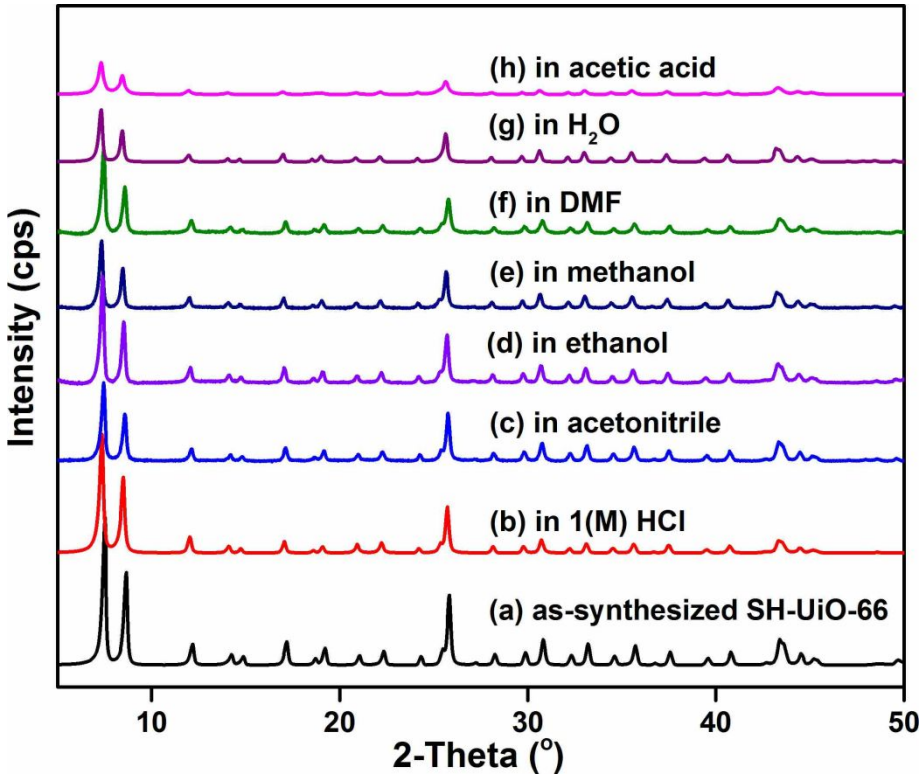

Figure S8. XRPD patterns of as-synthesized **SH-UiO-66** (a), in 1M HCl (b), in acetonitrile (c), in ethanol (d) in methanol (e), in DMF (f), in water (g) and in acetic acid (h).

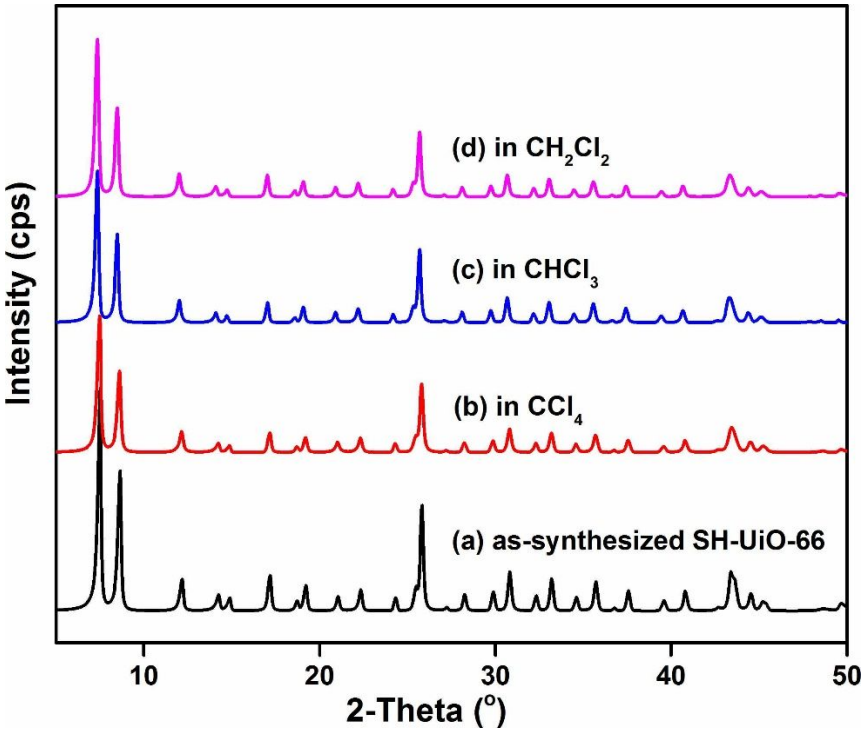

Figure S9. XRPD patterns of **SH-UiO-66** in different heavy oils.

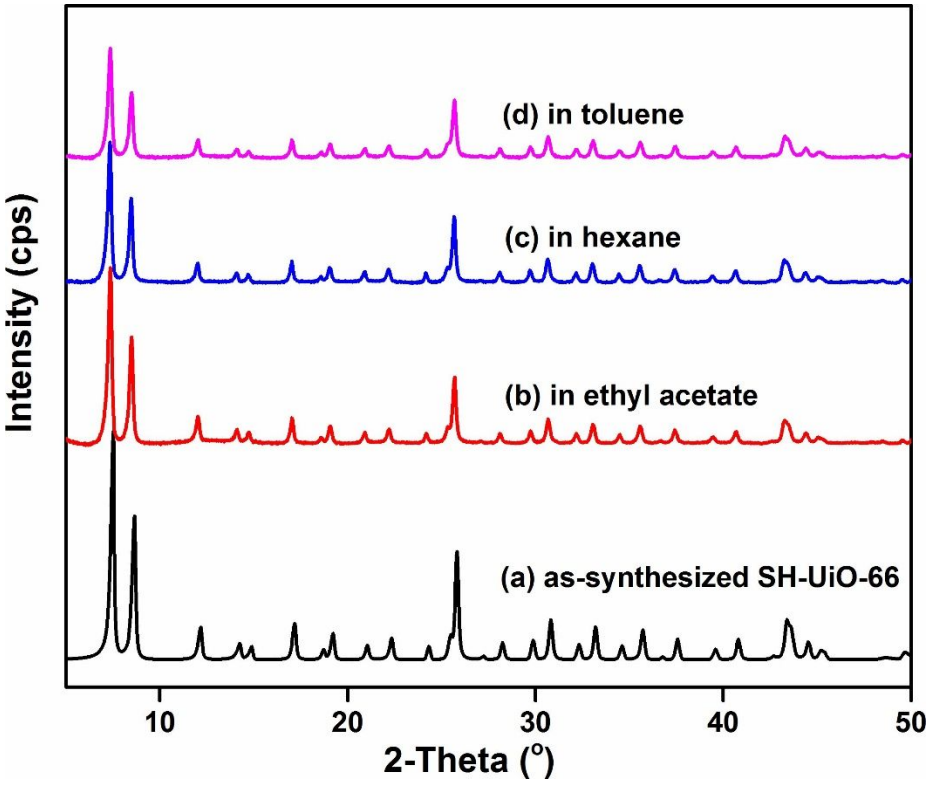

Figure S10. XRPD patterns of **SH-UiO-66** in different light oils.

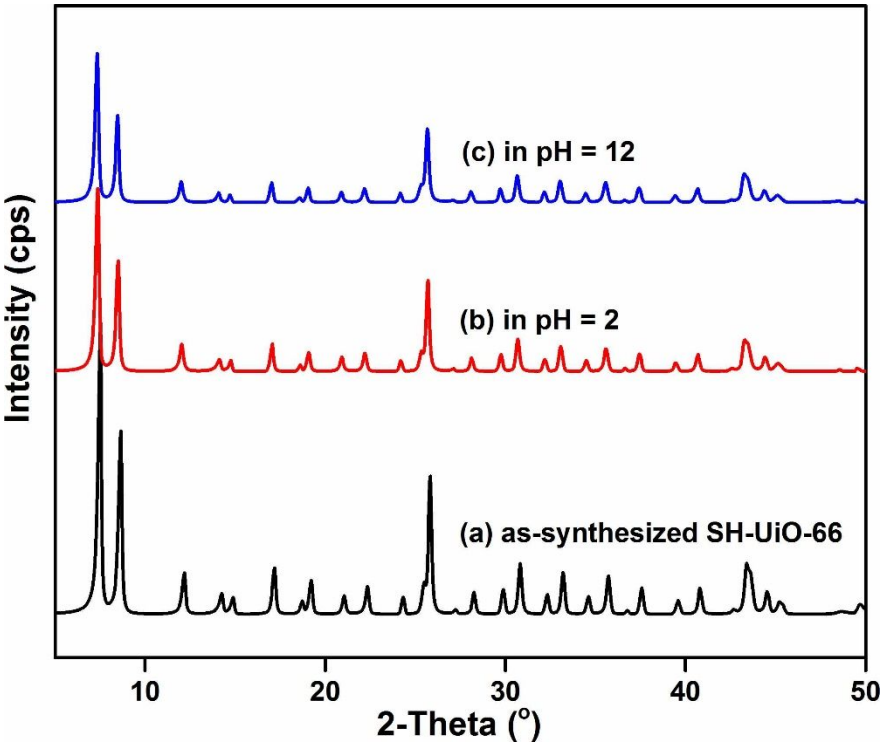

Figure S11. Aqua stability of **SH-UiO-66** in different pH media.

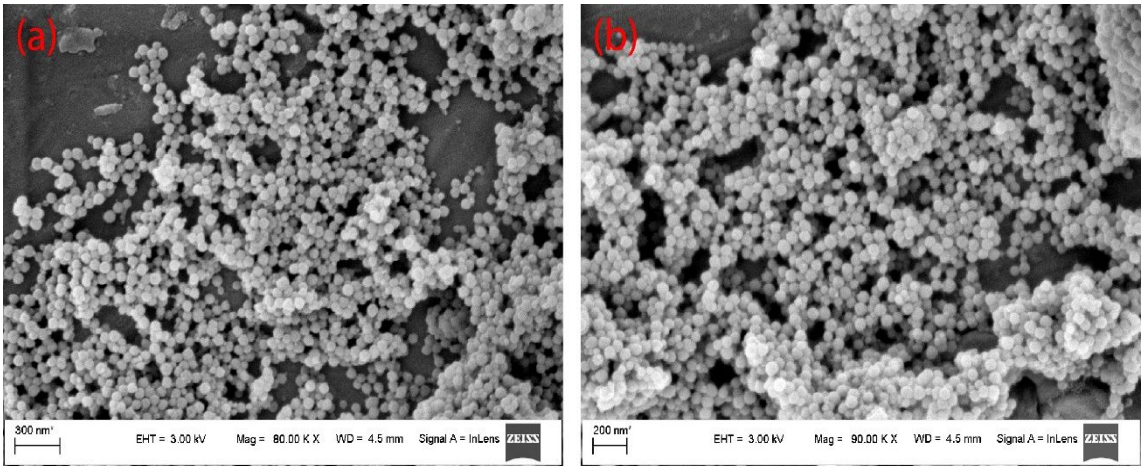

Figure S12. FE-SEM image of **SH-UiO-66** showing a homogeneous phase of monodispersed spherical particles, which suggest the phase purity of the material.

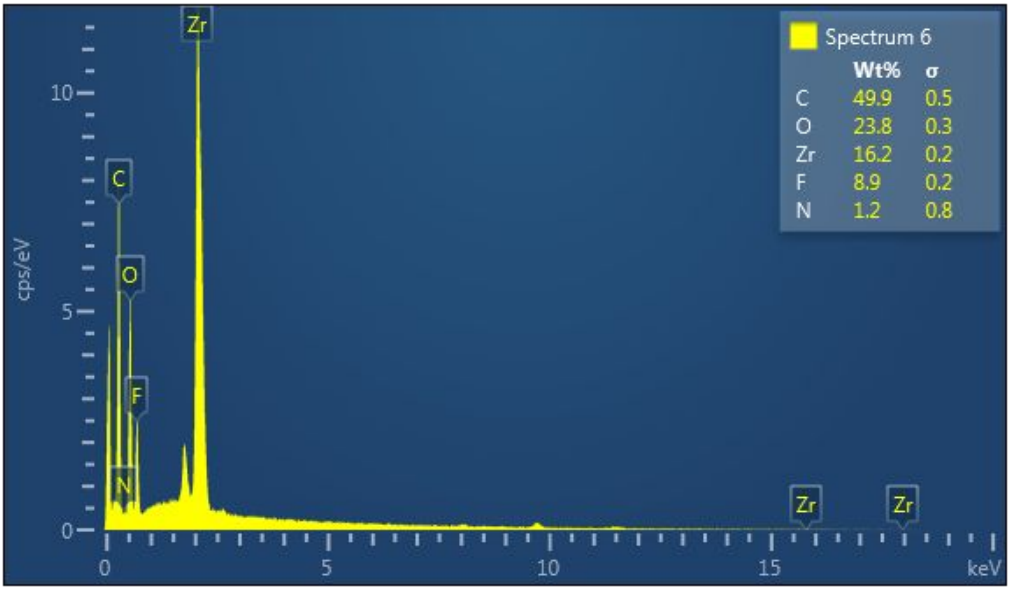

Figure S13. EDX spectrum of **SH-UiO-66**.

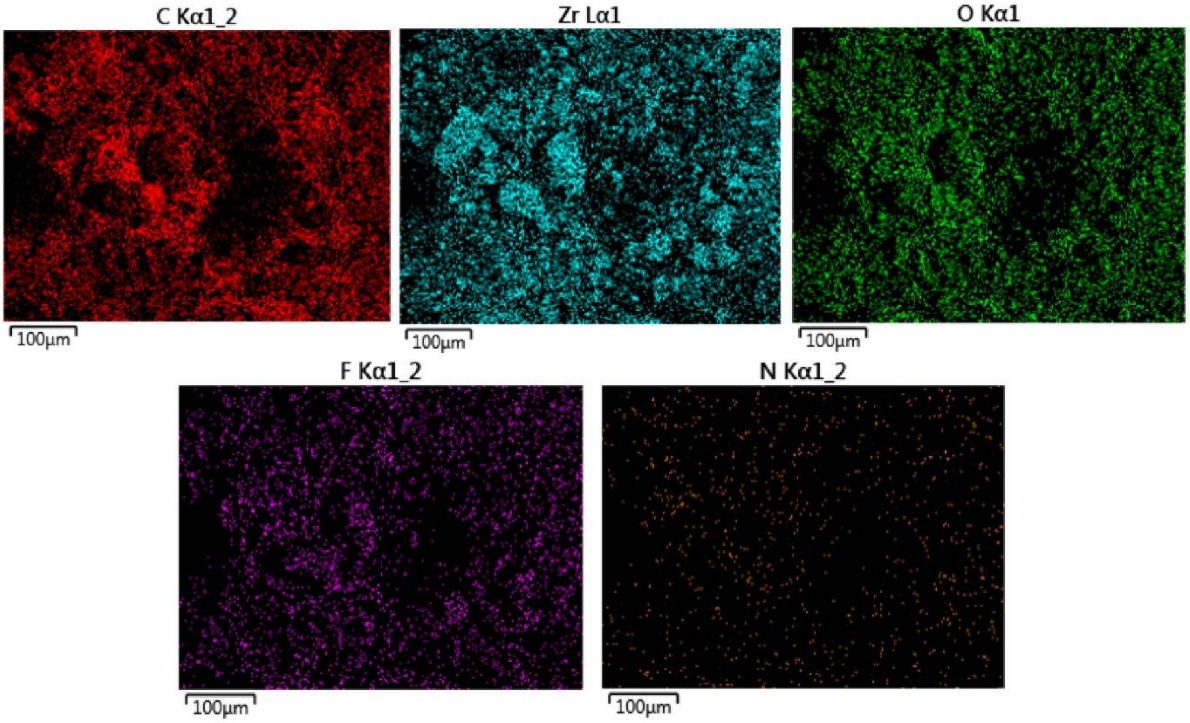

Figure S14. EDX elemental mapping of **SH-UiO-66**.

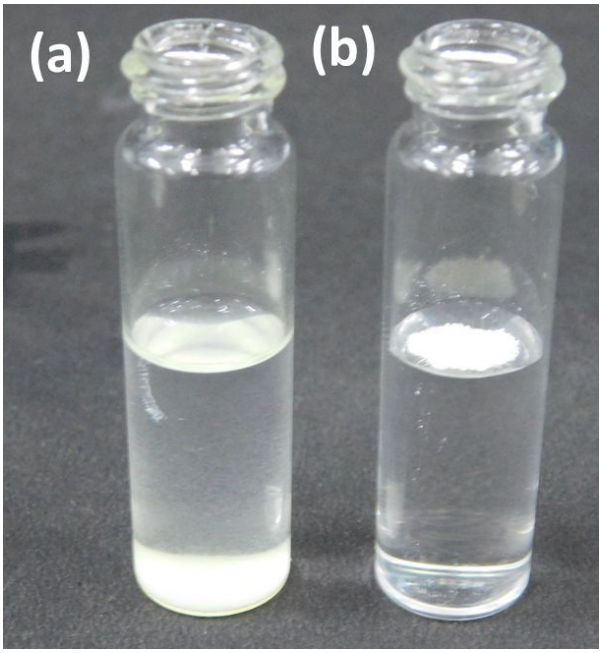

Figure S15. Self-floating ability of **SH-UiO-66**: in hexane (a) and in water (b).

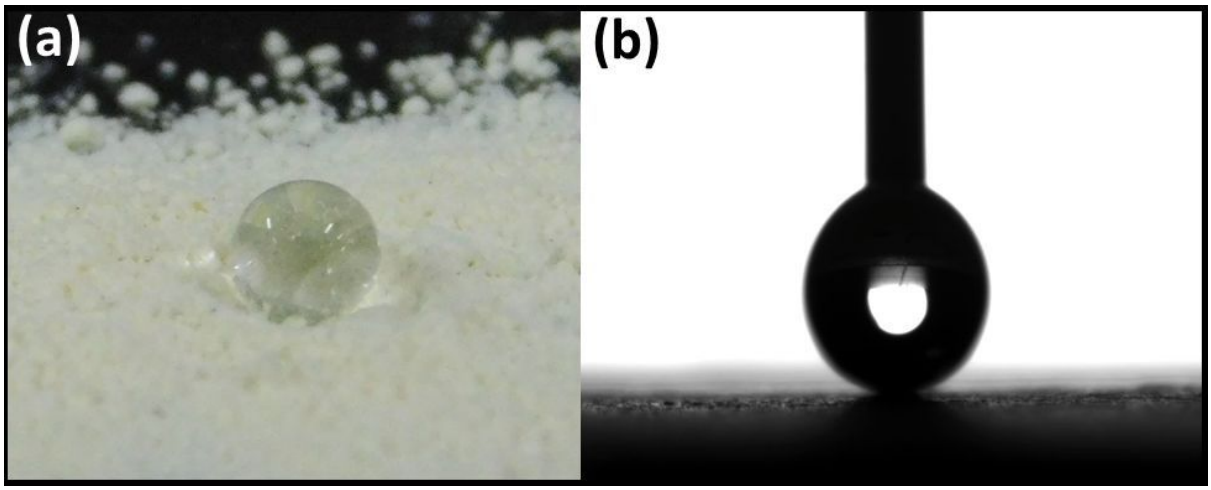

Figure S16. Water droplet suspended on **SH-UiO-66** MOF: naked eye proof of hydrophobicity (a); Image of a water droplet slowly cast on the hydrophobic surface of the **SH-UiO-66** MOF pellet with a contact angle of about 160° (b).

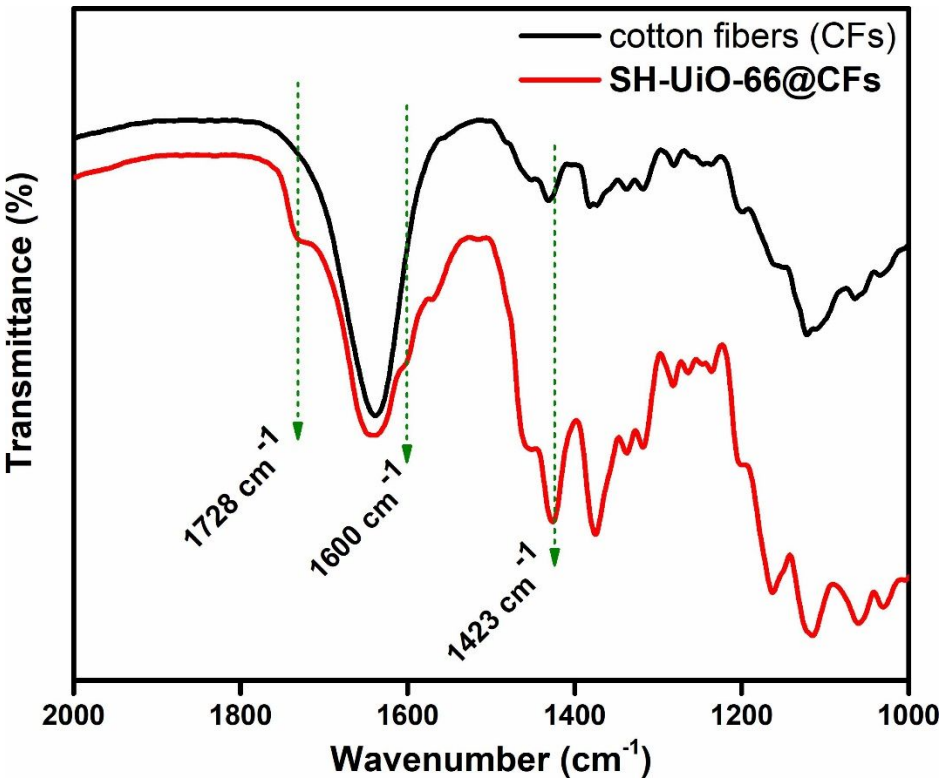

Figure S17. FT-IR spectra of cotton fibers and **SH-UiO-66@CFs** composite.

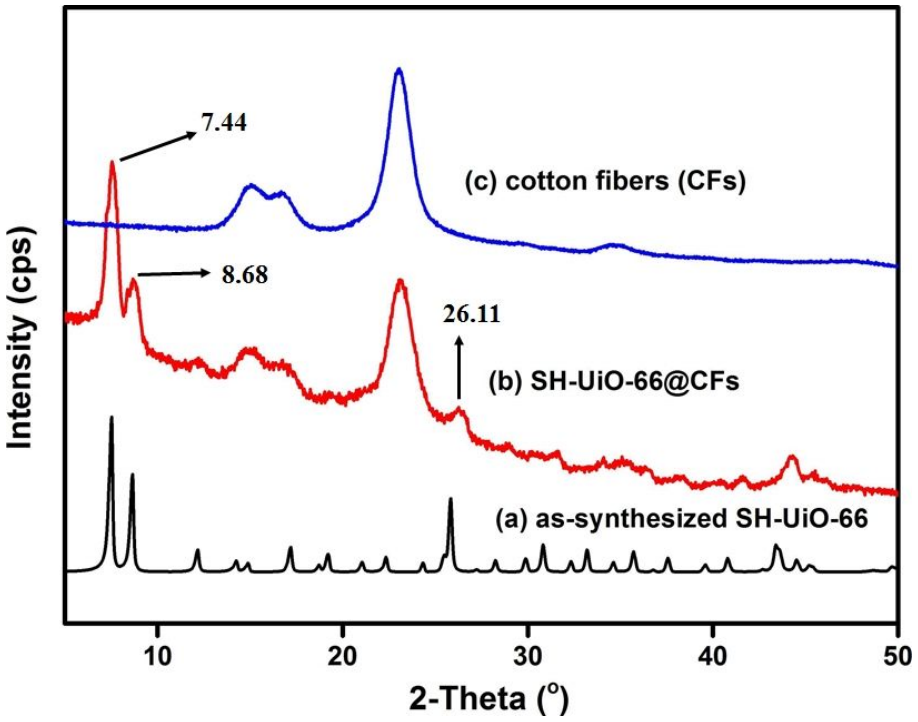

Figure S18. XRPD patterns of as-synthesized **SH-UiO-66**, **SH-UiO-66@@CFs** (b) and cotton fibers (c).

Figure S19. High resolution FE-SEM images of **SH-UiO-66@CFs**.

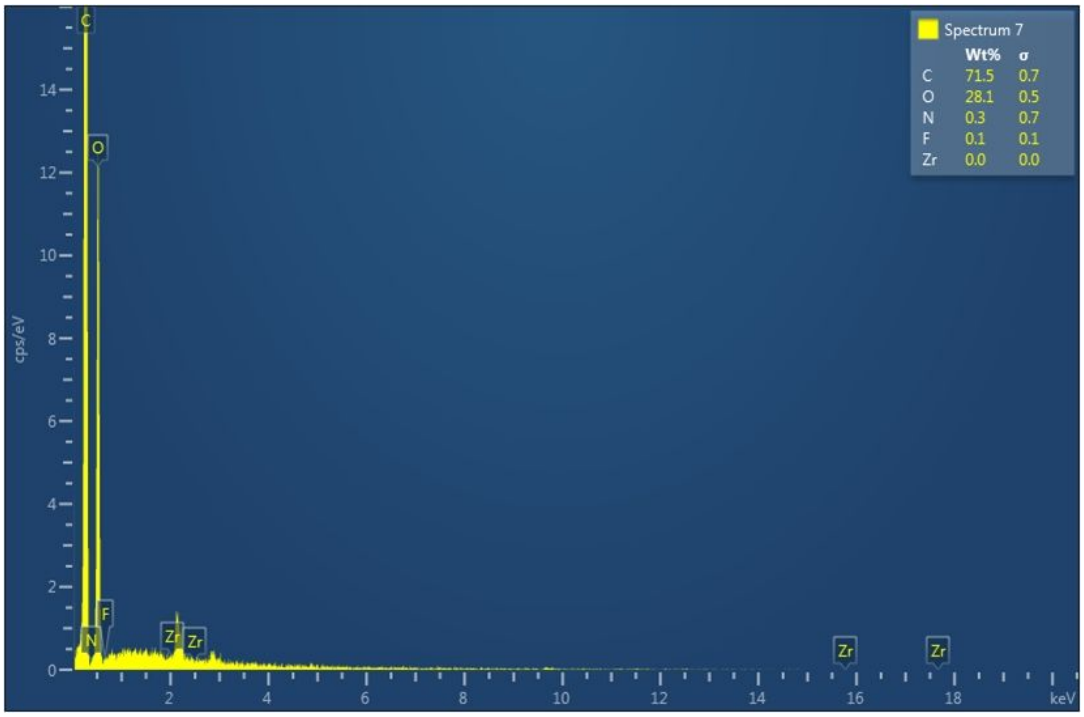

Figure S20. EDX spectrum of native cotton fiber.

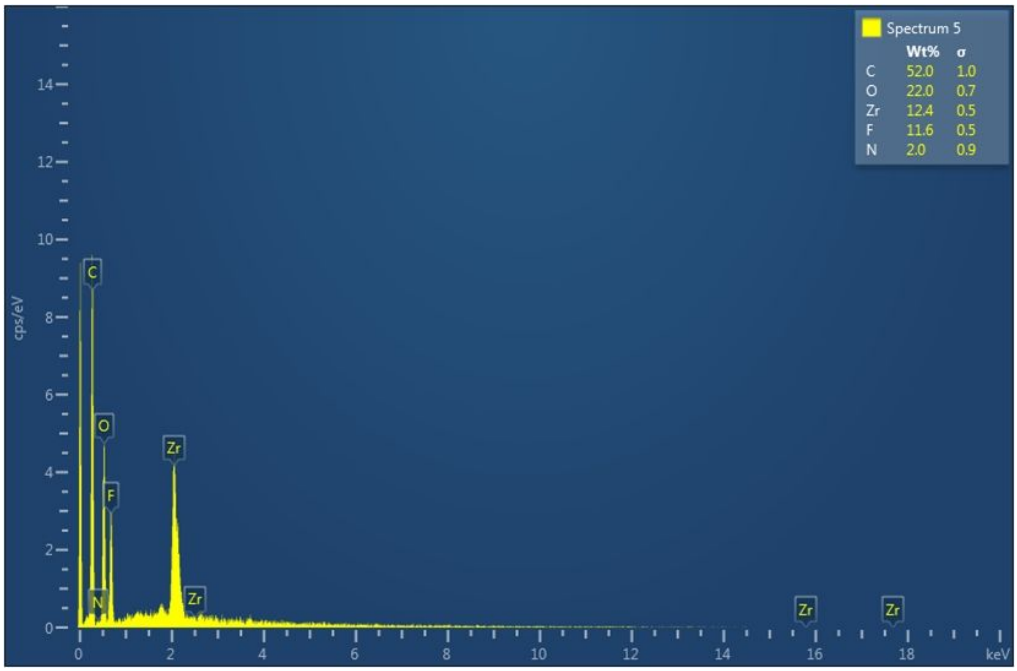

Figure S21. EDX spectrum of **SH-UiO-66@CFs**.

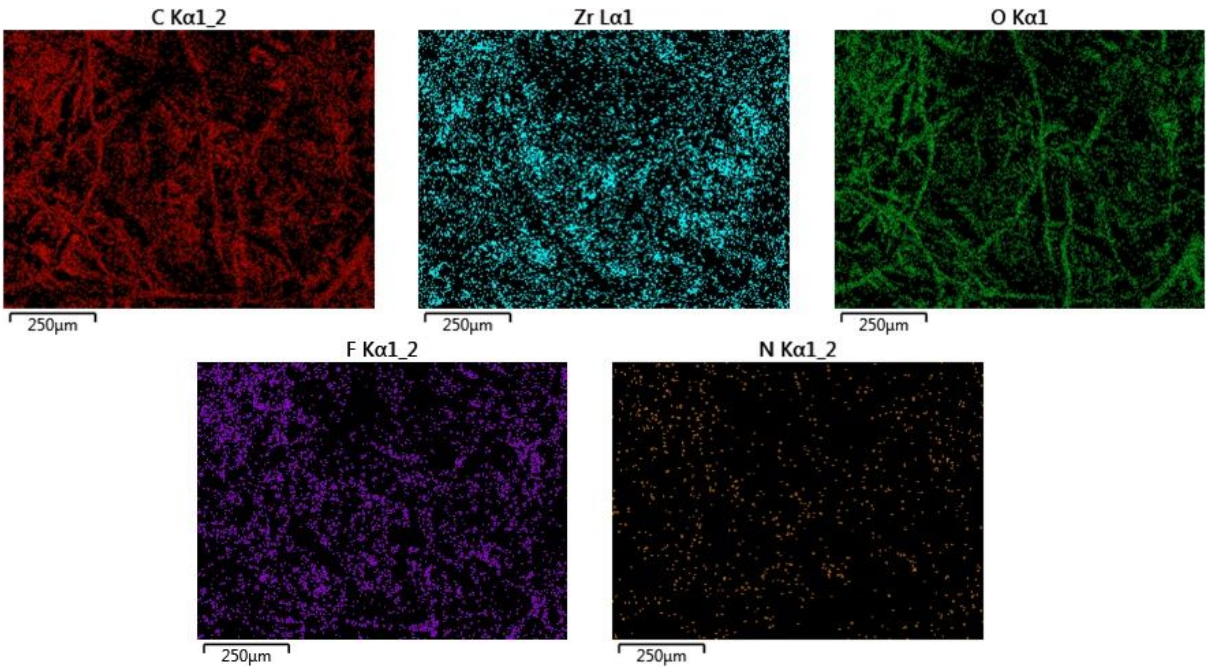

Figure S22. EDX elemental mapping of **SH-UiO-66@CFs**.

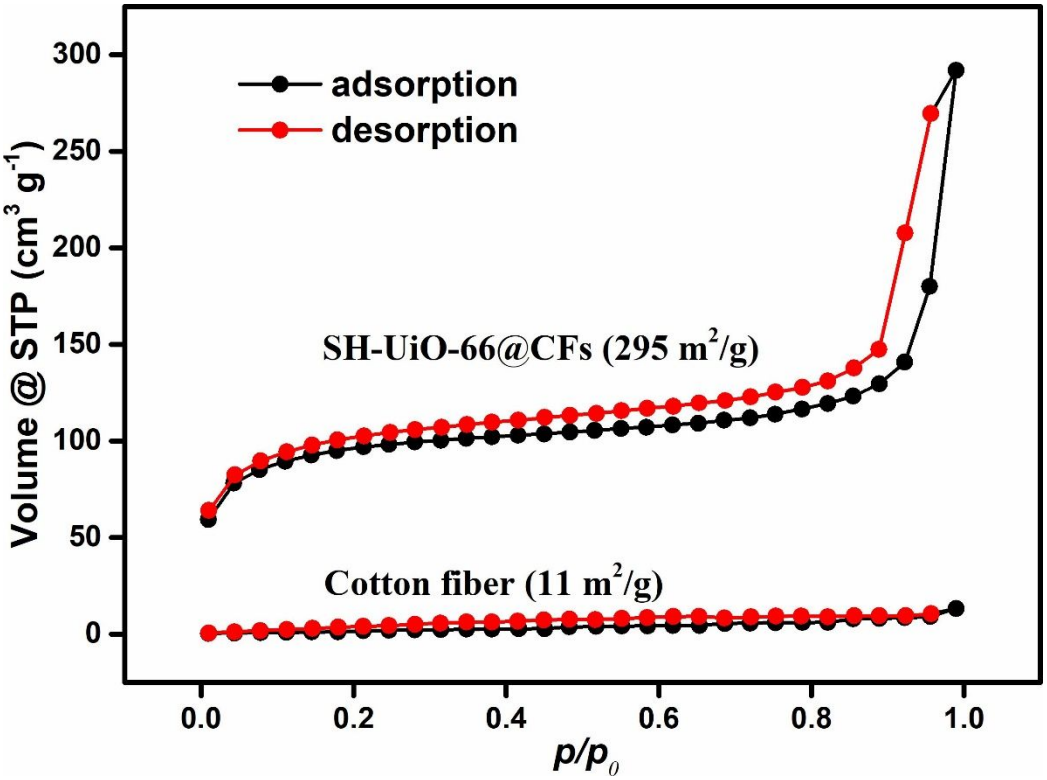

Figure S23. N_2 adsorption (black circles) and desorption (red circles) isotherms of **SH-UiO-66@CFs** and native cotton fiber recorded at –196 °C.

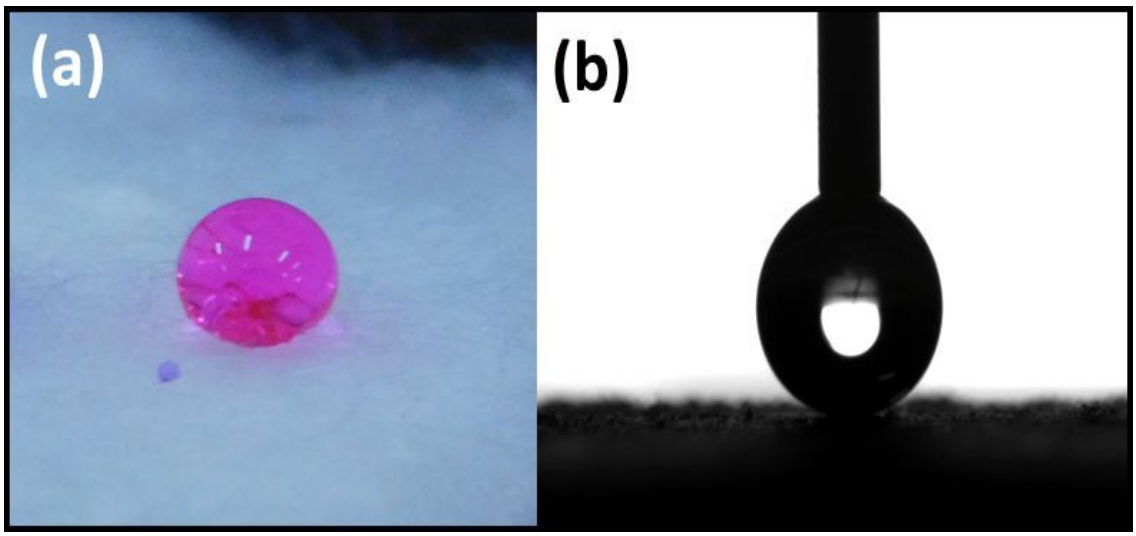

Figure S24. Water droplet (red colour aids visual inspection) suspended on **SH-UiO-66@CFs** composite: naked eye proof of hydrophobicity (a); Image of a water droplet slowly cast on the hydrophobic surface of the **SH-UiO-66@CFs** composite with a contact angle of about 163°.

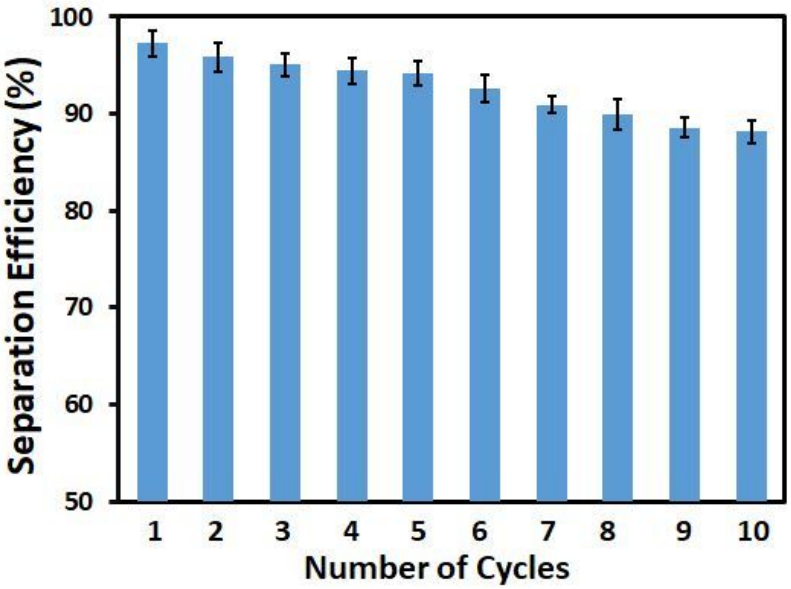

Figure S25. Reusability of **SH-UiO-66@CFs** composite for oil/water separation experiment (model oil: $CHCl_3$).

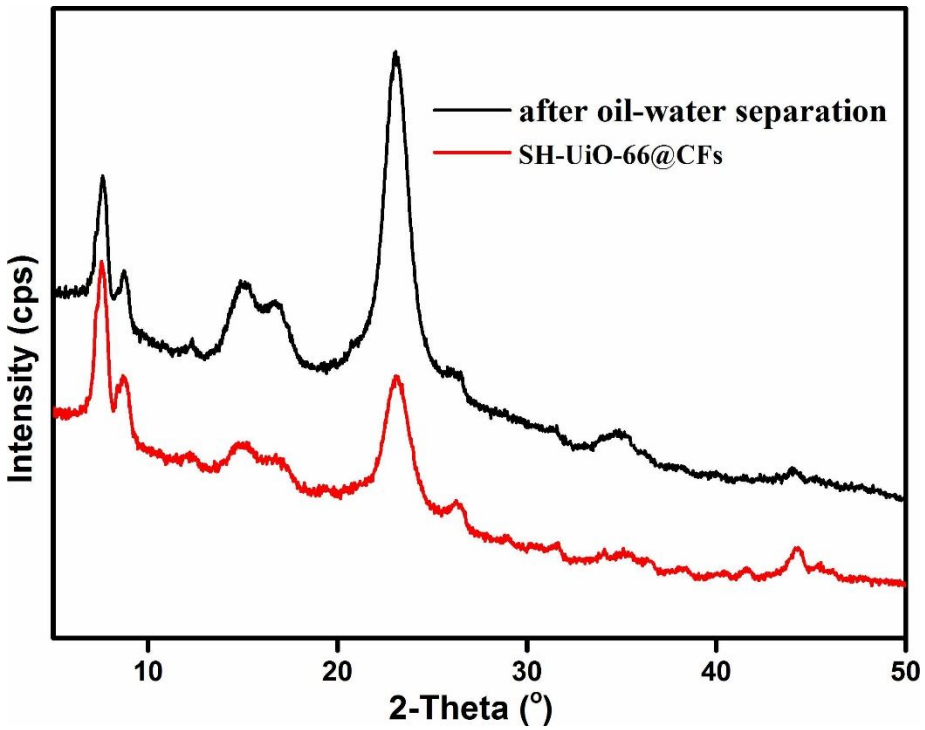

Figure S26. XRPD patterns of **SH-UiO-66@CFs** composite before (red) and after (black) oil-water separation experiments (model oil: $CHCl_3$).

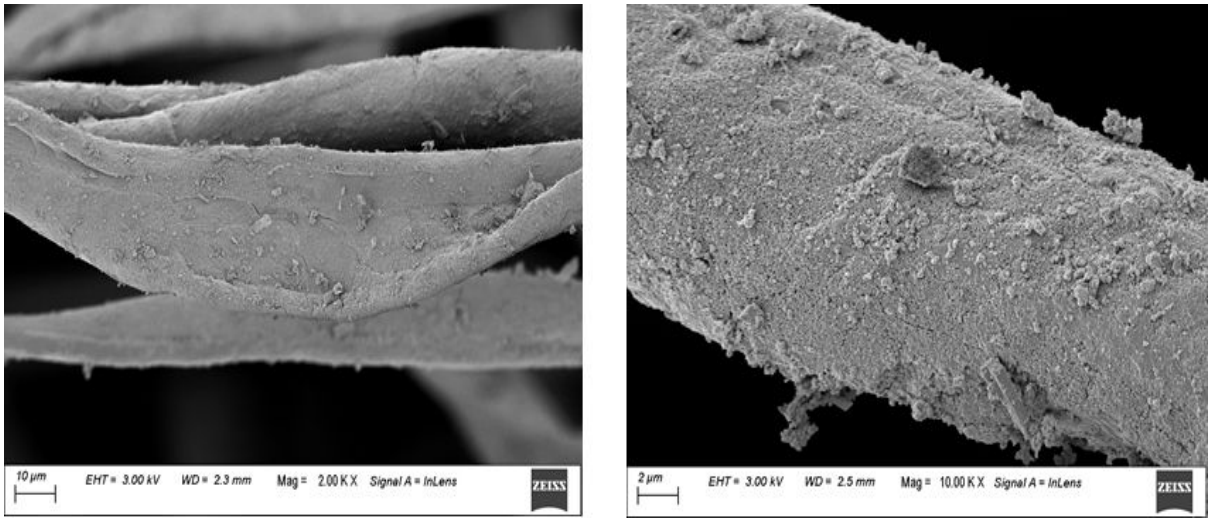

Figure S27. FE-SEM images of reused **SH-UiO-66@CFs** composite (model oil: $CHCl_3$).

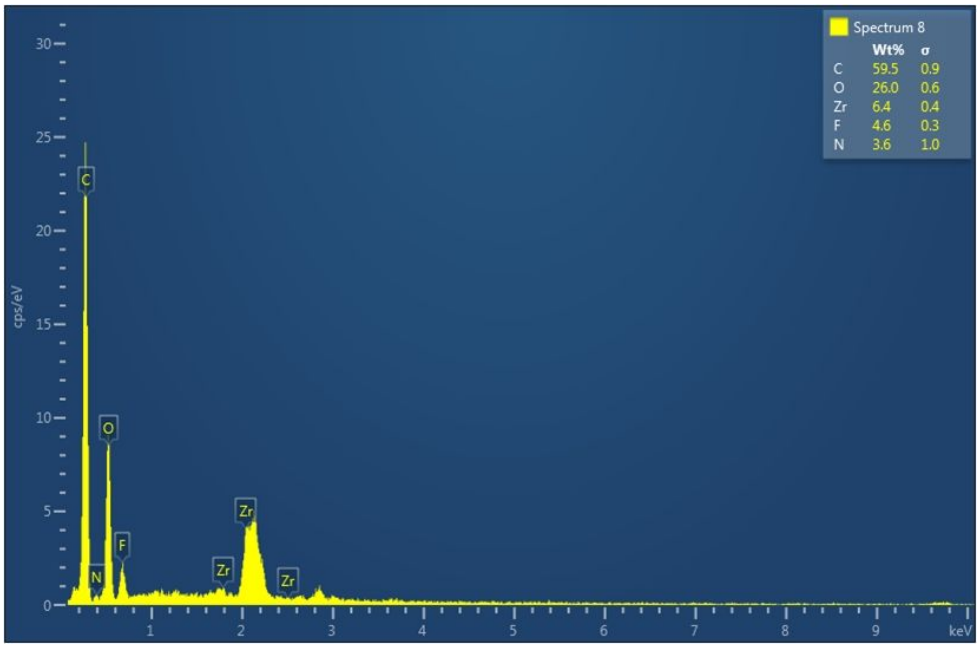

Figure S28. EDX spectrum of reused **SH-UiO-66@CFs** (model oil: $CHCl_3$).

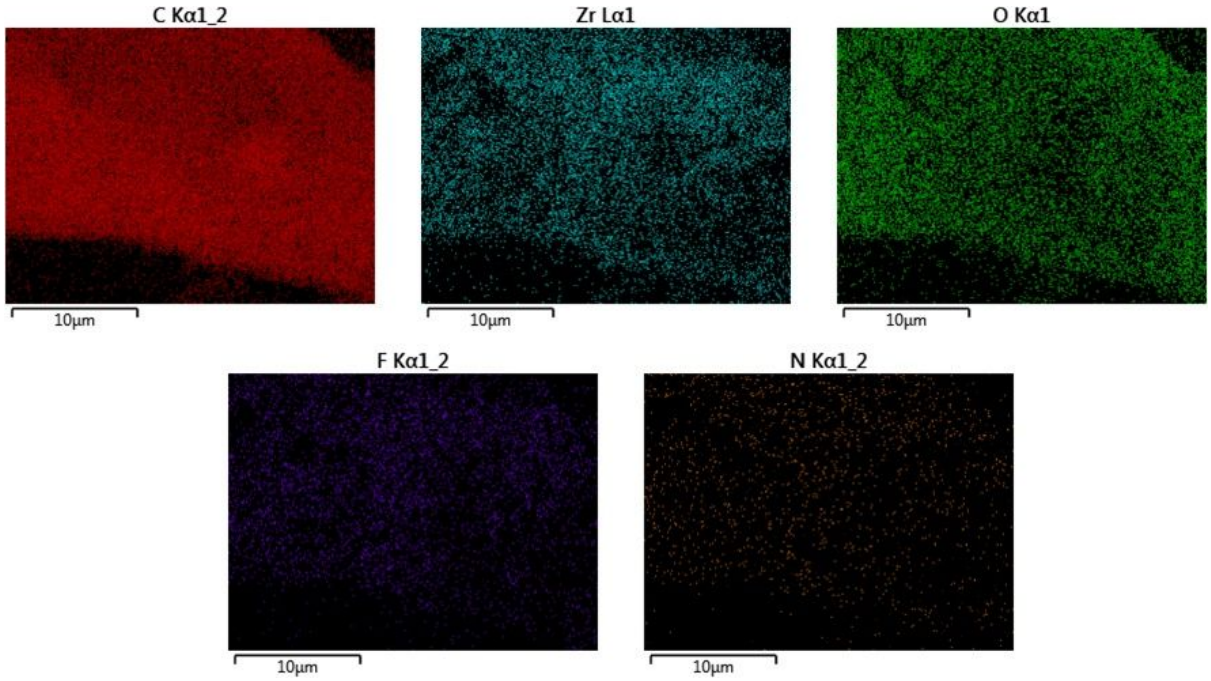

Figure S29. EDX elemental mapping of reused **SH-UiO-66@CFs** composite (model oil: $CHCl_3$).

Table S1. List of some reported hydrophobic MOFs, summarizing name of MOFs, WCA, constituent ligand, origin of hydrophobicity, investigated form and application.

Sl. No.	MOF	CA (in air) (deg)	Origin of hydrophobic nature	Investigation form	Applications	Ref.
1	SH-UiO-66	160	2-trifluoroacetamido terephthalic acid	MOF coated cotton fiber	recyclable oil/water separation (gravity driven, anti-gravity, under harsh conditions) and oil absorption	this work
2	PFOA@ UiO-67 & HFBA@ UiO-66	147 & 135	perfluorooctanoic acid (PFOA) and heptafluorobutyric acid (HFBA)	MOF powder	oil clean up from aqueous environment both under passive flow (column) and under simulated spill conditions	1
3	UHMOF-100	176	bis(trifluoromethyl) functionalized aromatic linker	crystalline powder	oil/water separation	2
4	ZIF-8@rGO@ Sponge	171	micro/nano-hierarchical architecture	composite sponge surface	recyclable oil/water separation	3

			comprising wrinkled, reduced rGO nano sheets intercalated with ZIF-8 nanoparticles			
5	NMOF-1	160-162, 171	H_2OPE-C_{18}	coated glass substrate	self cleaning	4-5
6	HFGO@ ZIF-8 composite	162	highly fluorinated graphene oxide (HFGO)	composite material pellet	oil/ water separation	6
7	OPA-UiO-66 & OPA-UiO-66-SO_3H & OPA-PCN-222	160 & 162 & 157	*n*-octa-decylphosphonic acid (OPA)	powder	high organic solvent absorption capacity; oil/water separation	7
8	PESD-1	152, >150	H_3BTMB	single crystal, powder	selective removal of organic solvent from water, benzene/ cyclohexane selective vapor sorption	8
9	fluorinated ZIF-90	152.4	pentalfluorobenzyla-mine	crystal	recyclable bio-alcohol recovery performance from water	9
10	MOFF-2	151±1	fluorinated biphenyl-based ligands	pressed crystal	N/A	10
11	SIM-2(C_{12})/Al_2O_3	>150	alkyl chain (C_{12})	film on Al_2O_3 support	catalyst for Knoevenagel condensation and CO_2/N_2 separation under humid conditions.	11
12	MIL-53(Al)-AM6 MIL-53(Al)-AM4 (AMn: Amide with *n*-carbon chain)	>150	hydrophobic alkyl chains	powder	N/A	12
13	FMOF-1	158	3,5-bis(trifluoromethyl)-1,2,4-triazolate	pellet	CO_2 selective gas sorption	13
14	PESD-1 PESD-2	155.5 159.3	H_3BTMB	powder	aromatic solvent adsorption;	14

	PESD-3	160.8			oil/water separation	

Table S2. Contact angle (CA) of **SH-UiO-66@CFs** after treatment under various conditions.

Sl. No.	**Treatment Conitions**	**CA (static)**
1	In dichloromethane (24 h)	163°
2	In chloroform (24 h)	151°
3	In carbon tetrachloride (24 h)	140°
4	In ethyl acetate (24 h)	154°
5	In hexane (24 h)	150°
6	In toluene (24 h)	151°
7	In tap water (24 h)	154°
8	In artificial sea water (24 h)	150°
9	In river water (24 h)	151°
10	In lake water (24 h)	152°
11	In pH = 2 (24 h)	152°
12	In pH = 12 (24 h)	148 °
13	In UV exposure (4 days)	155°
14	In ice water (24 h)	143°
14	In boiling water (24 h)	0°

Table S3. Density of oils used for oil/water separation experiments.

Sl. No.	**Oils**	**Density (g cm^{-3})**
1	dichloromethane	1.33
2	chloroform	1.49
3	carbon tetrachloride	1.59
4	ethyl acetate	0.90
5	hexane	0.65
6	toluene	0.86
7	motor oil	0.87
8	silicone oil	0.97
9	gasoline	0.78
10	kerosene	0.81

Table S4. Comparative absorption capacities of various absorbents for oil absorption.

Sl. No.	**Absorbents**	**Type of Oil**	**Absorption Capacity (g/g)**	**Ref.**
1	SH-UiO-66@CFs	motor oil silicone oil gasoline kerosene	45.23 38.06 31.87 29.41	this work
2	cotton fiber modified	diesel oil	25.61	15

	via the sol–gel method	lubrication oil crude oil	44.24 57.01	
3	modified jute fiber via the sol–gel method	crude oil diesel oil lubrication oil	7.41 8.48 10.29	16
4	mesoporous silica aerogel	petrol oil diesel oil	19.1 18.6	17
5	ultralight cellulose-based aerogel	pump oil diesel oil	22.60 20.9	18
6	i) cotton modified using P-SiO_2 nanoparticles ii) Kapok modified using P-SiO_2 nanoparticles	i) diesel oil ii) diesel oil	i) 20 ii) 23	19
7	PDMS-TiO_2-PU sponge	diesel oil	14.20	20
8	cellulose-based aerogels	crude oil diesel oil lubrication oil silicone oil	77.08 91.82 105.83 89.72	21
9	superhydrophobic/superoleophilic sawdust	crude oil	17.50	22

References:

1. DeChellis, D. M.; Ngule, C. M.; Genna, D. T., Removal of hydrocarbon contaminants from water with perfluorocarboxylated UiO-6X derivatives. *J. Mater. Chem. A* **2020,** *8*, 5848-5852.

2. Mukherjee, S.; Kansara, A. M.; Saha, D.; Gonnade, R.; Mullangi, D.; Manna, B.; Desai, A. V.; Thorat, S. H.; Singh, P. S.; Mukherjee, A.; Ghosh, S. K., An ultrahydrophobic fluorous metal–organic framework derived recyclable composite as a promising platform to tackle marine oil spills. *Chem. - Eur. J.* **2016,** *22*, 10937-10943.

3. Gu, J.; Fan, H.; Li, C.; Caro, J.; Meng, H., Back Cover: Robust superhydrophobic/superoleophilic wrinkled microspherical MOF@rGO composites for efficient oil–water separation. *Angew. Chem., Int. Ed.* **2019,** *58*, 5464-5464.

4. Roy, S.; Suresh, V. M.; Maji, T. K., Self-cleaning MOF: realization of extreme water repellence in coordination driven self-assembled nanostructures. *Chem. Sci.* **2016,** *7*, 2251-2256.

5. Samanta, D.; Roy, S.; Sasmal, R.; Saha, N. D.; Pradeep, K. R.; Ranjani, V.; Agasti, S. S.; Maji, T. K., Solvent adaptive dynamic metal-organic soft hybrid for imaging and biological delivery. *Angew. Chem., Int. Ed.* **2019,** *131*, 5062-5066.

6. Jayaramulu, K.; Datta, K. K. R.; Rösler, C.; Petr, M.; Otyepka, M.; Zboril, R.; Fischer, R. A., Biomimetic superhydrophobic/superoleophilic highly fluorinated graphene oxide and ZIF-8 composites for oil–water separation. *Angew. Chem., Int. Ed.* **2016,** *55*, 1178-1182.

7. Sun, Y.; Sun, Q.; Huang, H.; Aguila, B.; Niu, Z.; Perman, J. A.; Ma, S., A molecular-level superhydrophobic external surface to improve the stability of metal–organic frameworks. *J. Mater. Chem. A* **2017,** *5*, 18770-18776.

8. Rao, K. P.; Higuchi, M.; Sumida, K.; Furukawa, S.; Duan, J.; Kitagawa, S., Design of Superhydrophobic Porous Coordination Polymers through the Introduction of External Surface Corrugation by the Use of an Aromatic Hydrocarbon Building Unit. *Angew. Chem., Int. Ed.* **2014,** *53*, 8225-8230.

9. Liu, C.; Liu, Q.; Huang, A., A superhydrophobic zeolitic imidazolate framework (ZIF-90) with high steam stability for efficient recovery of bioalcohols. *Chem. Commun.* **2016,** *52*, 3400-3402.

10. Chen, T.-H.; Popov, I.; Zenasni, O.; Daugulis, O.; Miljanic, O. Š., Superhydrophobic perfluorinated metal–organic frameworks. *Chem. Commun.* **2013,** *49*, 6846-6848.

11. Aguado, S.; Canivet, J.; Farrusseng, D., Engineering structured MOF at nano and macroscales for catalysis and separation. *J. Mater. Chem.* **2011,** *21*, 7582-7588.

12. Nguyen, J. G.; S. M. Cohen, moisture-resistant and superhydrophobic metal−organic frameworks obtained via postsynthetic modification. *J. Am. Chem. Soc.* **2010,** *132*, 4560-4561.

13. Moghadam, P. Z.; Ivy, J. F.; Arvapally, R. K.; Santos, A. M. d.; Pearson, J. C.; Zhang, L.; Tylianakis, E.; Ghosh, P.; Oswald, I. W. H.; Kaipa, U.; Wang, X.; Wilson, A. K.; Snurr, R. Q.; Omary, M. A., Adsorption and molecular siting of CO_2, water, and other gases in the superhydrophobic, flexible pores of FMOF-1 from experiment and simulation. *Chem. Sci.* **2017,** *8*, 3989-4000.

14. Rao, K. P.; Higuchi, M.; Suryachandram, J.; Kitagawa, S., Temperature-stable compelled composite superhydrophobic porous coordination polymers achieved via an unattainable de novo synthetic method. *J. Am. Chem. Soc.* **2018,** *140*, 13786–13792.

15. Lv, N.; Wang, X.; Peng, S.; Luo, L.; Zhou, R., Superhydrophobic/superoleophilic cotton-oil absorbent: preparation and its application in oil/ water separation. *RSC Adv.* **2018,** *8*, 30257-30264.

16. Lv, N.; Wang, X.; Peng, S.; Zhang, H.; Luo, L., Study of the kinetics and equilibrium of the adsorption of oils onto hydrophobic jute fiber modified via the sol-gel method. *Int. J. Environ. Res. Public Health* **2018,** *15*, 969.

17. Zhang, C.; Dai, C.; Zhang, H.; Peng, S.; Wei, X.; Hu, Y., Regeneration of mesoporous silica aerogel for hydrocarbon adsorption and recovery. *Mar. Pollut. Bull.* **2017,** *122*, 129-138.
18. Zhang, H.; Li, Y.; Xu, Y.; Lu, Z.; Chen, L.; Huang, L.; Fan, M., Versatile fabrication of a superhydrophobic and ultralight cellulose-based aerogel for oil spillage clean-up. *Phys. Chem. Chem. Phys.* **2016,** *18*, 28297-28306.
19. Lee, J. H.; Kim, D. H.; Han, S. W.; Kim, B. R.; Park, E. J.; Jeong, M.-G.; Kim, J. H.; Kim, Y. D., Fabrication of superhydrophobic fibre and its application to selective oil spill removal. *Chem. Eng. J.* **2016,** *289*, 1-6.
20. Shuai, Q.; Yang, X.; Luo, Y.; Tang, H.; Luo, X.; Tan, Y.; Ma, M., A superhydrophobic poly(dimethylsiloxane)-TiO_2 coated polyurethane sponge for selective absorption of oil from water. *Mater. Chem. Phys.* **2015,** *162*, 94-99.
21. Yin, T.; Zhang, X.; Liu, X.; Wang, C., Resource recovery of Eichhornia crassipes as oil superabsorbent. *Mar. Pollut. Bull.* **2017,** *118*, 267-274.
22. Zang, D.; Liu, F.; Zhang, M.; Gao, Z.; Wang, C., Novel superhydrophobic and superoleophilic sawdust as a selective oil sorbent for oil spill cleanup. *Chem. Eng. Res. Des.* **2015,** *102*, 34-41.